Inorganic Chemistry
Article

Inorg. Chem. **2009**, *48*, 10257–10263 **10257**
DOI: 10.1021/ic9013587

H_2 Activation by a (PNP)Ir(C_6H_5) Complex via the Dearomatization/Aromatization Process of the PNP Ligand: A Computational Study

Guixiang Zeng, Yong Guo, and Shuhua Li*

School of Chemistry and Chemical Engineering, Key Laboratory of Mesoscopic Chemistry of Ministry of Education, Institute of Theoretical and Computational Chemistry, Nanjing University, Nanjing, 210093, P. R. China

Received July 12, 2009

Density functional theory calculations have been carried out to explore the mechanism of the H_2 activation by the (PNP)Ir(C_6H_5) complex. Our calculations show that the reaction is most likely to go though three steps. The first step (also the rate-determining step) involves the proton transfer from the benzylic position of the PNP ligand to the metal center to form an Ir(III) hydride intermediate, accompanied by the dearomatization of the PNP ligand. Second, H_2 is coordinated to the metal of this Ir(III) intermediate to form a molecular hydrogen complex. Finally, the H−H bond is heterolytically cleaved to produce the final trans-dihydride product, in which the benzylic carbon is protonated, and the PNP ligand is rearomatized. Thus, the H_2 activation by the Ir(I) complex actually involves an Ir(III) hydride complex as a key intermediate. The Ir center and the PNP ligand cooperate in a synergistic manner in the H_2 activation process. The above molecular mechanism could provide reasonable explanations for known experimental facts.

1. Introduction

A number of experimental and theoretical studies have shown that some bond activation reactions may involve the cooperation of the metal center and its surrounding ligands.[1−23] For example, the activation of H_2 by [Cp*$_2$(py)Ti=S] is promoted by a Ti=S double bond.[24] In 2006, Milstein et al. reported that the PNP ligand and the metal work cooperatively via the dearomatization/aromatization processes of the PNP ligand in the activation of H_2 by a (PNP)Ir(C_6H_5) complex.[25] In their experiment, one equiv of H_2 reacts with (PNP)Ir(C_6H_5) at room temperature in benzene, producing the trans-dihydride complex (PNP)Ir(H)$_2$(C_6H_5) exclusively (Scheme 1). When D_2 is used instead, the only product is the compound (PNP)Ir(H)(D)(C_6H_5) with one deuterium being at the benzylic "arm", other than the trans-dideuteride complex (PNP)Ir(D)(D)(C_6H_5). It has been suggested that during the H_2 activation process the reactant (PNP)Ir(C_6H_5) may first convert into a transient Ir(III) hydride intermediate, then this intermediate may react with H_2 to give the final product (Scheme 2).[25] This intermediate, with the dearomatized

*E-mail: shuhua@nju.edu.cn.

(1) Jørgensen, C. K. *Coord. Chem. Rev.* **1966**, *1*, 164–178.
(2) Matt, P. V.; Pfaltz, A. *Angew. Chem., Int. Ed. Engl.* **1993**, *32*, 566–568. *Angew. Chem.* **1993**, *105*, 614−615.
(3) Rieck, H.; Helmchen, G. *Angew. Chem., Int. Ed. Engl.* **1995**, *34*, 2687–2689. *Angew. Chem.* **1995**, *107*, 2881−2883.
(4) Yamakawa, M.; Ito, H.; Noyori, R. *J. Am. Chem. Soc.* **2000**, *122*, 1466–1478.
(5) Braunstein, P.; Naud, F. *Angew. Chem., Int. Ed.* **2001**, *40*, 680–699. *Angew. Chem.* **2001**, *113*, 702−722.
(6) Noyori, R.; Koizumi, M.; Ishii, D.; Ohkuma, T. *Pure Appl. Chem.* **2001**, *73*, 227–232.
(7) Pfaltz, A.; Blankenstein, J.; Hilgraf, R.; Hörmann, E.; McIntyre, S.; Menges, F.; Schönleber, M.; Smidt, S. P.; Wüstenberg, B.; Zimmermann, N. *Adv. Synth. Catal.* **2003**, *345*, 33.
(8) Braunstein, P. *J. Organomet. Chem.* **2004**, *689*, 3953–3967.
(9) Clapham, S. E.; Hadzovic, A.; Morris, R. H. *Coord. Chem. Rev.* **2004**, *248*, 2201–2237.
(10) Abbel, R.; Abdur-Rashid, K.; Faatz, M.; Hadzovic, A.; Lough, A. J.; Morris, R. H. *J. Am. Chem. Soc.* **2005**, *127*, 1870–1882.
(11) Casey, C. P.; Bikzhanova, G. A.; Cui, Q.; Guzei, I. L. *J. Am. Chem. Soc.* **2005**, *127*, 14062–14071.
(12) Comas-Vives, A.; Ujaque, G.; Lleds, A. *Organometallics* **2007**, *26*, 4135–4144.
(13) Gibson, V. C.; Redshaw, C.; Solan, G. A. *Chem. Rev.* **2007**, *107*, 1745–1776.
(14) Helmchen, G.; Dahnz, A.; Dübon, P; Schelwies, M.; Weihofen, R. *Chem. Commun.* **2007**, 675–691.
(15) Zotto, A. D.; Baratta, W.; Ballico, M.; Herdtweck, E.; Rigo, P. *Organometallics* **2007**, *26*, 5636–5642.
(16) Benito-Garagorri, D.; Kirchner, K. *Acc. Chem. Res.* **2008**, *41*, 201–213.
(17) Grützmacher, H. *Angew. Chem., Int. Ed.* **2008**, *47*, 1814–1818. *Angew. Chem.* **2008**, *120*, 1838−1842.
(18) Hesp, K. D.; McDonald, R.; Ferguson, M. J.; Stradiotto, M. *J. Am. Chem. Soc.* **2008**, *130*, 16394–16406.
(19) Yang, X.; Hall, M. B. *J. Am. Chem. Soc.* **2008**, *130*, 1798–1799.
(20) Friedrich, A.; Ghosh, R.; Kolb, R.; Herdtweck, E.; Schneider, S. *Organometallics* **2009**, *28*, 708–718.
(21) Choualeb, A.; Lough, A. J.; Gusev, D. G. *Organometallics* **2007**, *26*, 3509–3515.
(22) Rankin, M. A.; Schatte, G.; McDonald, R.; Stradiotto, M. *Organometallics* **2008**, *27*, 6286–6299.
(23) Tejel, C.; Ciriano, M. A.; Hetterscheid, D. G. H.; Spithas, N. T. i.; Smits, J. M. M.; Bruin, B. d. *Chem. Eur. J.* **2008**, *14*, 10932–10936.
(24) Sweeney, Z. K.; Polse, J. L.; Bergman, R. G.; Andersen, R. A. *Organometallics* **1999**, *18*, 5502–5510.
(25) Ben-Ari, E.; Leitus, G.; Shimon, L. J. W.; Milstein, D. *J. Am. Chem. Soc.* **2006**, *128*, 15390–15391.

Published on Web 09/28/2009

Scheme 1. Activation of H_2 by the Complex (PNP)Ir(C_6H_5)[25]

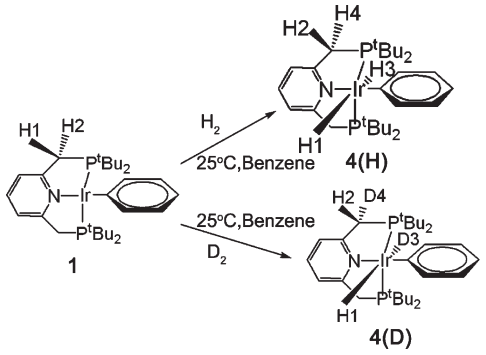

Scheme 2. Possible Pathway for H_2 Activation by the Complex (PNP)Ir(C_6H_5)

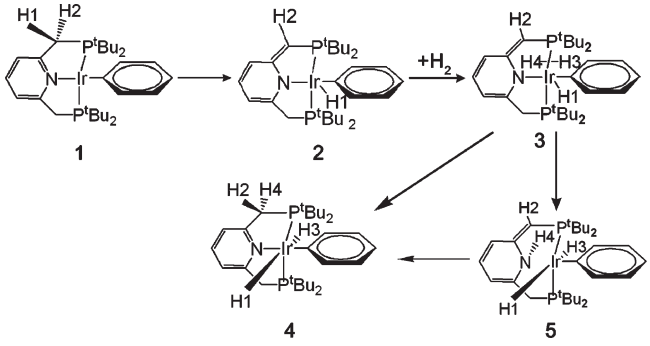

pyridine ring, is assumed to be generated by the migration of one of the benzylic hydrogens to the metal center. In fact, the dearomatization/aromatization process of the pyridine ring in the PNP or similar PNN ligand was proposed to be a key step in many other reactions.[26−33]

Up to now, the mechanistic details of the H_2 activation by (PNP)Ir(C_6H_5) have not been studied theoretically. Here, we carry out detailed density functional theory (DFT) calculations to explore the possible reaction pathways for this H_2 activation. The results from our calculations can reasonably account for the observed experimental facts.

2. Computational Details

The calculations were carried out using the B3LYP[34,35] hybrid density functional method implemented in the Gaussian03 program.[36] The effective core potential LANL2DZ[37] was employed for Ir, and a modified LANL2DZ basis set with the optimized 6p functions from Couty and Hall[38] and a set of f-type functions[39] (Table S2) was used for Ir. The 6-31G basis set is used for twelve methyl groups, and the 6-31++G** basis set is used for the rest of the atoms. All the stationary points along the reaction coordinate are determined to have singlet ground states (see Table S1 in the Supporting Information). For each stationary point, a frequency calculation is done to check out whether it is a minimum or a transition state and to obtain its Gibbs free energy. In addition, intrinsic reactions coordinate (IRC)[40] calculations are done to verify whether a transition state is truly connecting the reactant and the product. The solvation free energy for each species is calculated at the gas-phase optimized geometry, using the polarizable-continuum model (PCM)[41] with benzene as the solvent. For each species, the free energy in the solvent is obtained as the sum of its gas-phase free energy and the solvation free energy.

For the rate-determining steps, we also perform DFT calculations with several other functionals such as TPSS,[42] TPSSh,[43] BMK,[44] M05,[45] and PBE,[46] since they were shown to provide improved reaction barriers in some cases.[47−50] The structures of the corresponding stationary points are fully optimized with each functional, and then vibrational frequencies are carried out to obtain free energy barriers in both gas phase and the solvent.

3. Results and Discussions

In this section, the potential energy surfaces of two reaction pathways (pathway I (Scheme 2) and II (Scheme 3)) have been explored. Pathway I has been described earlier in the introduction, in which the H−H bond activation occurs after the dearomatization process of the PNP ligand. However, we think, another reaction channel (pathway II) should also be considered. Along this pathway, the first step is the oxidative addition of H_2 to the metal to form a cis-dihydride intermediate, followed by a series of steps to produce the trans-dihydride product. A detailed description on pathway II

(26) Gunanathan, C.; Ben-David, Y.; Milstein, D. *Science* **2007**, *317*, 790–792.
(27) Hanson, S. K.; Heinekey, D. M.; Goldberg, K. I. *Organometallics* **2008**, *27*, 1454–1463.
(28) Kloek, S. M.; Heinekey, D. M.; Goldberg, K. I. *Angew. Chem., Int. Ed.* **2007**, *46*, 4736–4738. *Angew. Chem.* **2007**, *119*, 4820−4822.
(29) Trovitch, R. J.; Lobkovsky, E.; Chirik, P. J. *Inorg. Chem.* **2006**, *45*, 7252–7260.
(30) Vlugt, J. I. v. d.; Lutz, M.; Pidko, E. A.; Vogta, D.; Spekb, A. L. *Dalton Trans.* **2009**, *6*, 1016–1023.
(31) Vlugt, J. I. v. d.; Pidko, E. A.; Vogt, D.; Lutz, M.; Spek, A. L.; Meetsma, A. *Inorg. Chem.* **2008**, *47*, 4442–4444.
(32) Vuzman, D.; Poverenov, E.; Shimon, L. J. W.; Diskin-Posner, Y.; Milstein, D. *Organometallics* **2008**, *27*, 2627–2634.
(33) Zhang, J.; Gandelman, M.; Shimon, L. J. W.; Milstein, D. *Dalton Trans.* **2007**, *5*, 107–113.
(34) Becke, A. D. *J. Chem. Phys.* **1993**, *98*, 5648–5652.
(35) Lee, C.; Yang, W.; Parr, R. G. *Phys. Rev. B* **1988**, *37*, 785–789.
(36) Frisch, M. J.; Trucks, G. W.; Schlegel, H. B.; Scuseria, G. E.; Robb, M. A.;Cheeseman, J. R.; Montgomery, J. A., Jr.; Vreven, T.; Kudin, K. N.; Burant, J. C.; Millam, J. M.; Iyengar, S. S.; Tomasi, J.; Barone, V.; Mennucci, B.; Cossi, M.; Scalmani, G.; Rega, N.; Petersson, G. A.; Nakatsuji, H.; Hada, M.; Ehara, M.; Toyota, K.; Fukuda, R.; Hasegawa, J.; Ishida, M.; Nakajima, T.; Honda, Y.; Kitao, O.; Nakai, H.; Klene, M.; Li, X.; Knox, J. E.; Hratchian, H. P.; Cross, J. B.; Adamo, C.; Jaramillo, J.; Gomperts, R.; Stratmann, R. E.; Yazyev, O.; Austin, A. J.; Cammi, R.; Pomelli, C.; Ochterski, J. W.; Ayala, P. Y.; Morokuma, K.; Voth, G. A.; Salvador, P.; Dannenberg, J. J.; Zakrzewski, V. G.; Dapprich, S.; Daniels, A. D.; Strain, M. C.; Farkas, O.; Malick, D. K.; Rabuck, A. D.; Raghavachari, K.; Foresman, J. B.; Ortiz, J. V.; Cui, Q.; Baboul, A. G.; Clifford, S.; Cioslowski, J.; Stefanov, B. B.; Liu, G.; Liashenko, A.; Piskorz, P.; Komaromi, I.; Martin, R. L.; Fox, D. J.; Keith, T.; Al-Laham, M. A.; Peng, C. Y.; Nanayakkara, A.; Challacombe, M.; Gill, P. M. W.; Johnson, B.; Chen, W.; Wong, M. W.; Gonzalez, C.; Pople, J. A. A. *Gaussian 03, Revision B.04*; Gaussian Inc.: Wallingford, CT, 2004.
(37) Hay, P. J.; Wadt, W. R. *J. Chem. Phys.* **1985**, *82*, 299–310.
(38) Couty, M.; Hall, M. B. *J. Comput. Chem.* **1996**, *17*, 1359–1370.
(39) Ehler, A. W.; Böhme, M.; Dapprich, S.; Gobbi, A.; Höllwarth, A.; Jonas, V.; Köhler, K. F.; Segmann, R.; Velkamp, A.; Frenking, G. *Chem. Phys. Lett.* **1993**, *208*, 111–114.
(40) Gonzalez, C.; Schlegel, H. B. *J. Chem. Phys.* **1989**, *90*, 2154–2161.
(41) Tomasi, J.; Persico, M. *Chem. Rev.* **1994**, *94*, 2027–2094.
(42) Tao, J.; Perdew, J. P. *Phys. Rev. Lett.* **2003**, *91*, 146401–146404.
(43) Staroverov, V. N.; Scuseria, G. E.; Tao, J.; Perdew, J. P. *J. Chem. Phys.* **2003**, *119*, 12129–12137.
(44) Boese, A. D.; Martin, J. M. L. *J. Chem. Phys.* **2004**, *121*, 3405–3416.
(45) Zhao, Y.; Schultz, N. E.; Truhlara, D. G. *J. Chem. Phys.* **2005**, *123*, 161103–161106.
(46) Perdew, J. P.; Burke, K.; Ernzerhof, M. *Phys. Rev. Lett.* **1996**, *77*, 3865–3868.
(47) Harvey, J. N. *Annu. Rep. Prog. Chem., Sect. C* **2006**, *102*, 203–226.
(48) Sousa, S. r. F.; Fernandes, P. A.; Ramos, M. J. o. *J. Phys. Chem. A* **2007**, *111*, 10439–10452.
(49) Zhao, Y.; Truhlar, D. G. *J. Phys. Chem. A* **2006**, *110*, 10478–10486.
(50) Furche, F.; Perdew, J. P. *J. Chem. Phys.* **2006**, *124*, 044103–044129.

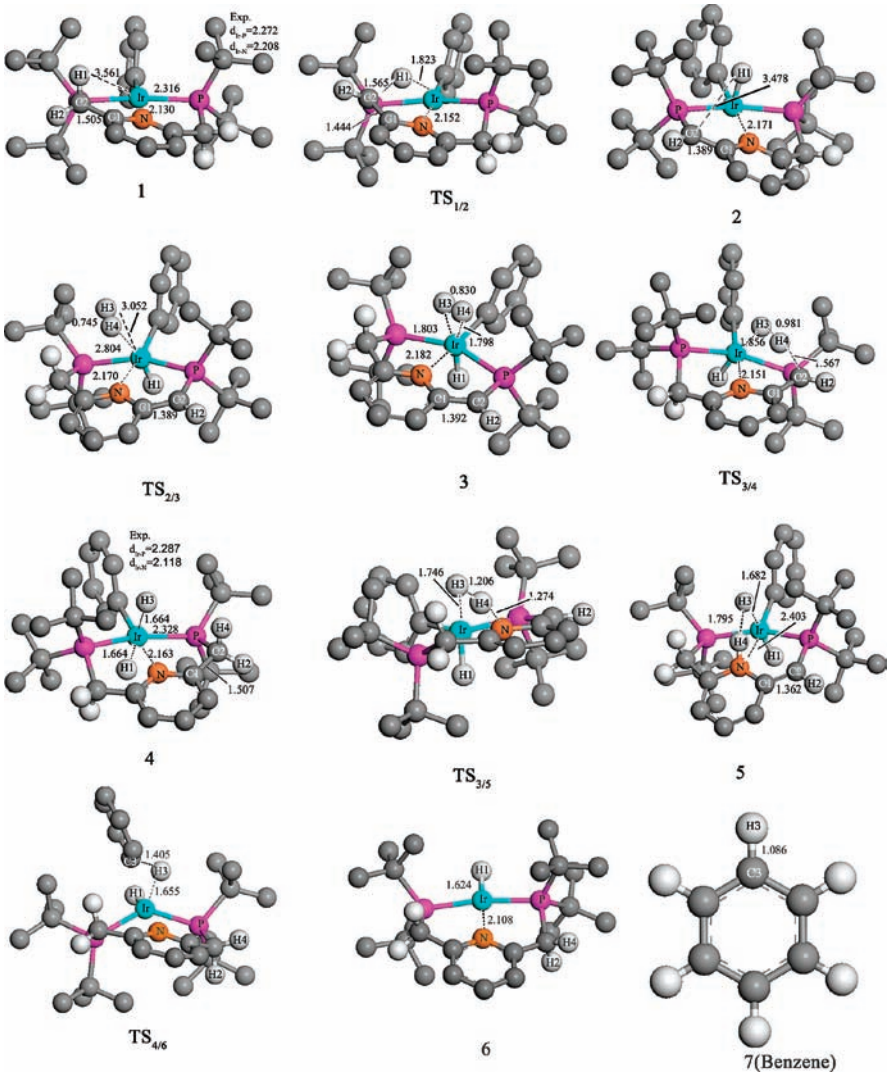

Figure 1. Optimized structures of stationary points along the pathway I. All the distances are in Å. All hydrogen atoms are omitted for clarity (except those involved in the H_2 activation).

Scheme 3. Pathway II for H_2 Activation by the Complex (PNP)Ir(C_6H_5)

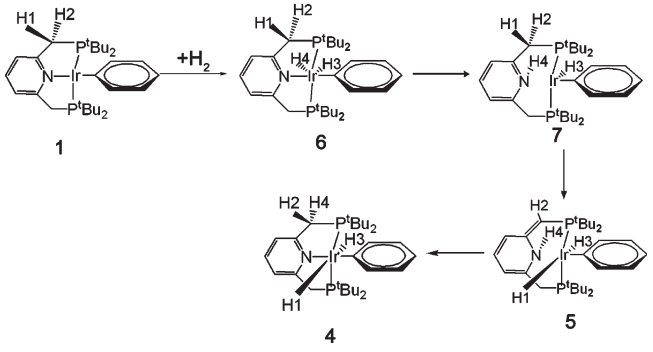

(Scheme 3) will be given later in this section. For both pathways, we have explored the potential energy profiles for both the singlet and triplet states. Since the triplet state surface is significantly higher than the singlet surface (see Table S1), we only discuss the results on the singlet surface.

3.1. The Potential Energy Profile of Pathway I. The optimized structures of all the stationary points along this pathway (Scheme 2) are displayed in Figure 1, and the Gibbs free energy profiles (in the gas phase and in the solvent) are presented in Figure 2. Calculated electronic energies, zero-point energy (ZPE) corrected energies, and solvation free energies for all species are provided in the Supporting Information (Table S1). Although the solvation free energy has an insignificant influence on the potential energy profile, free energies obtained in the solvent will be used exclusively in discussing the reaction pathways.

Along this pathway, the first step is the transfer of one of the benzylic hydrogens to the Ir center to form a metal hydride intermediate **2**. In the reactant **1**, the distance between the Ir center and one of the benzylic hydrogens (H1) is 3.561 Å. The PNP ligand is slightly distorted from the planar geometry, and the pyridine ring has an aromatic structure. The calculated Ir−N and Ir−P distances are 2.130 and 2.316 Å, respectively, being in good agreement with the data from the X-ray crystal structure.[25] In **2**, the C1−C2 distance is 1.389 Å, indicating a double bond. The geometrical parameters of the pyridine ring show a dearomatized structure. We have successfully located the proton transfer transition state, $\mathbf{TS_{1/2}}$, which connects **1** and **2**. In $\mathbf{TS_{1/2}}$, the distances of C2−H1 and

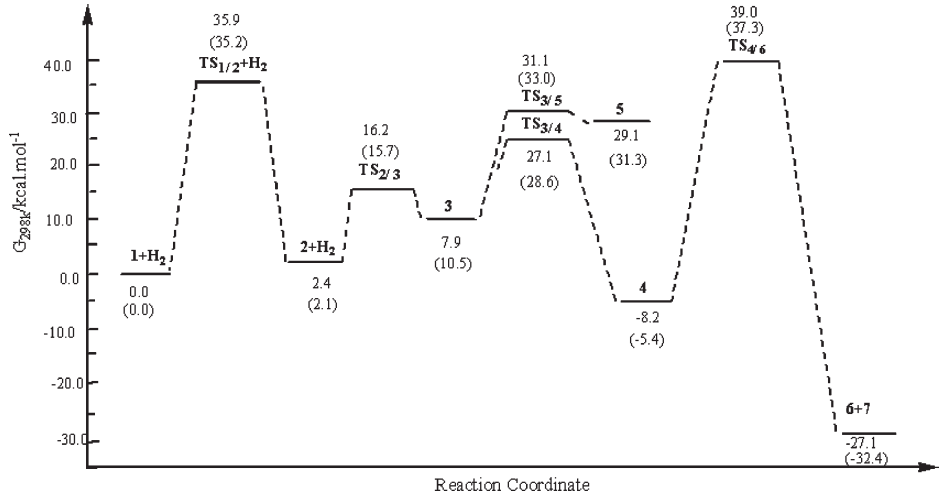

Figure 2. Gibbs free energy profiles in the solvent of the pathway I. Free energies in gas phase are presented in parentheses.

H1−Ir are 1.565 Å and 1.823 Å, respectively. The C1−C2 distance (1.444 Å) shows a strong double bond character. The structure of this transition state also shows that the transfer of the benzylic hydrogen (H1) to the Ir center is accompanied by the dearomatization process of the pyridine ring. This structural change is understandable since the dearomatization process of the pyridine ring could help stabilize the radical center C2. Energetically, the Ir(III) hydride intermediate **2** is only about 2.4 kcal/mol above **1**. The free energy barrier for this step is 35.9 kcal/mol. To get a more accurate barrier, we perform single point calculations with a larger basis set for the reactant **1** and the transition state $\mathbf{TS_{1/2}}$. The obtained free energy barrier is 35.1 kcal/mol in the solvent (the results are collected in Table S2). This barrier is still relatively high for a reaction to occur at room temperature.

In order to get a more reliable evaluation on the barrier of this step, we have also reoptimized the structures of species **1** and $\mathbf{TS_{1/2}}$ using functionals TPSS, TPSSh, BMK, M05, and PBE with the same basis set (the structures of these two species are collected in Figures S1−S4). The free energy barriers in the solvent are calculated to be 31.9 (TPSS), 33.6 (TPSSh), 32.6 (BMK), 34.7 (M05), and 30.3 kcal/mol (PBE). Thus, all these functionals give similar results as the hybrid B3LYP functional.

One may wonder whether there exists an alternative pathway (with lower energy) for the transfer of the benzylic hydrogen to the metal. The most likely one is that the benzylic hydrogen may first migrate to the nitrogen of the amide group, and then this hydrogen migrates to the Ir center. However, our calculations demonstrate that the hypothetic intermediate with the N−H bond is not a minimum on the potential energy surface. So this reaction channel can be excluded.

A possible explanation for the observed high rate of this step is that the migration of the benzylic hydrogen to the metal center could occur by a hydrogen tunneling process.[51−54] In 2008, Schreiner and his co-workers reported that the rearrangement of hydroxymethylene to formaldehyde (with an activation barrier of about 30 kcal/mol) could occur at 11 K by pure hydrogen tunneling.[55,56] In the experiments, species **2** can quantitatively convert to **1** after 10 h at −50 °C.[25] This fact shows that **1** is thermodynamically slightly more stable than **2**, which is supported by the results described above. Moreover, it was observed experimentally that the transformation of species **2a** (with the deuteride ligand) into **1a** (with a D-labeled benzyl "arm") occurred only at room temperature.[25] This fact suggests that at room temperature the deuterium may also migrate from the benzylic arm to the metal center via a tunneling process.

Table 1. Natural Atomic Charges on Atoms Involved in the H−H Cleavage Process

	3	$\mathbf{TS_{3/4}}$	4
Ir	0.09	0.11	0.08
H3	0.05	−0.17	−0.25
H4	0.06	0.19	0.27
C2	−0.84	−0.88	−0.81

In the second step, H_2 coordinates to the Ir center of species **2** via $\mathbf{TS_{2/3}}$ to form a molecular hydrogen complex **3**. In $\mathbf{TS_{2/3}}$, the H3−H4 distance is 0.745 Å. It is almost the same as that (0.744 Å) in free dihydrogen. The two Ir−H distances are 2.804 and 3.052 Å, respectively. In **3**, the molecular hydrogen is significantly activated, since the H3−H4 distance is 0.830 Å, and the Ir−H3 (Ir−H4) distance is 1.803 Å (1.798 Å). This step is endothermic by 5.5 kcal/mol and has a free energy barrier of 13.8 kcal/mol. Since the ZPE-corrected energy barrier of this step is only 5.5 kcal/mol, one can see that most of the free energy barrier comes from the loss of translation and rotation entropies from H_2.

From **3**, H4 could directly transfer to the benzylic position of the PNP ligand through the transition state $\mathbf{TS_{3/4}}$, generating the trans-dihydride product **4**. The product **4** is thermodynamically more stable than the reactants ($\mathbf{1} + H_2$) by 8.2 kcal/mol. In $\mathbf{TS_{3/4}}$, the C2−H4 distance is 1.567 Å, the H3−H4 distance is 0.981 Å, and the Ir−H3 distance is

(51) Caldin, E. F. *Chem. Rev.* **1969**, *69*, 135–156.
(52) Kohen, A.; Cannio, R; Bartolucci, S.; Klinman, J. P. *Nature* **1999**, *399*, 496–499.
(53) Rucker, J.; Klinman, J. P. *J. Am. Chem. Soc.* **1999**, *121*, 1997–2006.
(54) Tresadern, G.; McNamara, J. P.; Mohr, M.; Wang, H; A.Burton, N.; Hillier, I. H. *Chem. Phys. Lett.* **2002**, *358*, 489–494.
(55) Bucher, G. *Angew. Chem., Int. Ed.* **2008**, *47*, 6957–6958. *Angew. Chem.* **2008**, *120*, 7064−7065.
(56) Schreiner, P. R.; Reisenauer, H. P.; Pickard, F. C., IV; Simmonett, A. C.; Allen, W. D.; Mátyus, E.; Császár, A. G. *Nature* **2008**, *453*, 906–909.

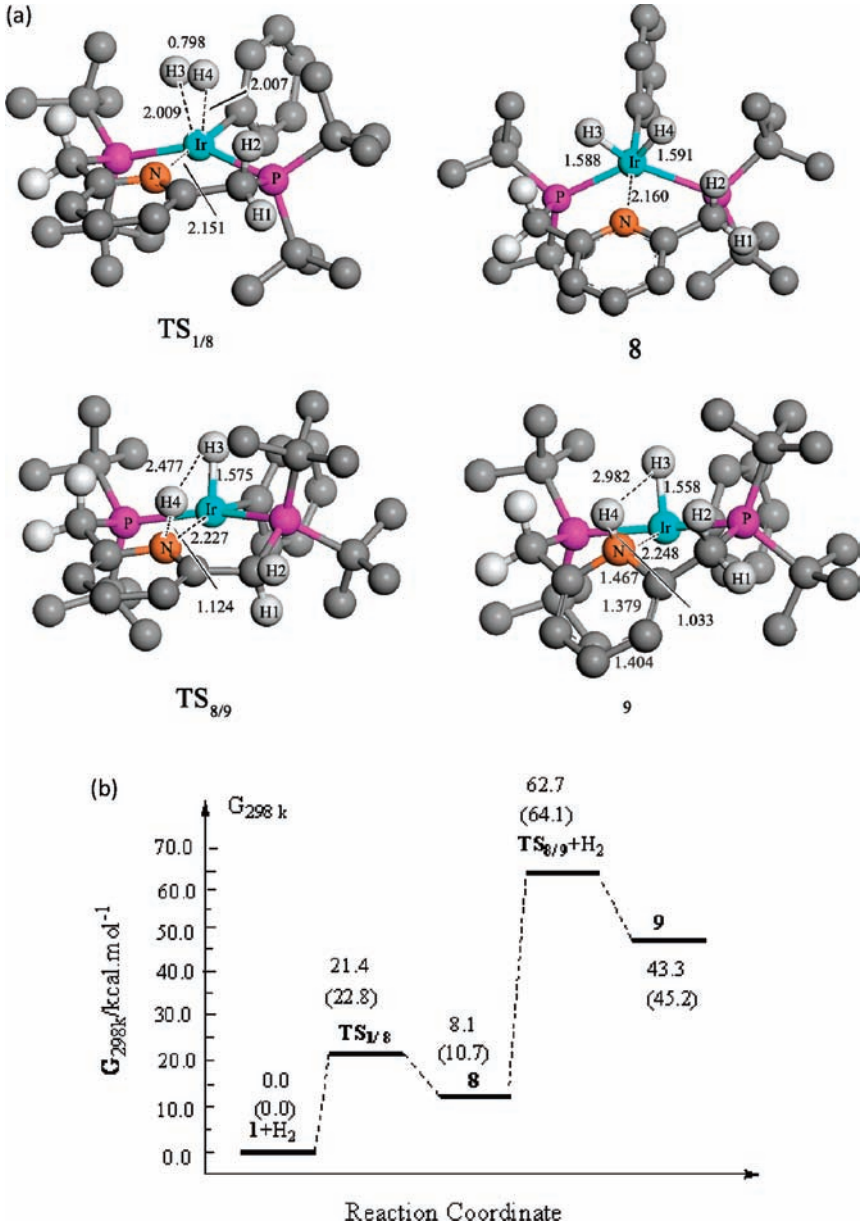

Figure 3. (a) Optimized structures of some stationary points along pathway II. The distances are in Å. All hydrogen atoms are omitted for clarity (except those involved in the H_2 activation). (b) Gibbs free energy profile (from **1**+H_2 to **9**) in the solvent of pathway II. Free energies in gas phase are presented in parentheses.

1.856 Å. As shown in Table 1, the natural atomic charge on H4 increases from 0.06e in **3** to 0.19e in $\mathbf{TS_{3/4}}$ and to 0.27e in **4**. Meanwhile, the natural atomic charge on H3 gradually decreases from 0.05e in **3** to −0.17e in $\mathbf{TS_{3/4}}$ and to −0.25e in **4**. The data clearly show that the H3−H4 bond is heterolytically cleaved. The structural parameters of the product **4** deserve some comments. The C1−C2 distance is now 1.507 Å, and the aromatic structure is restored for the pyridine ring. The calculated geometrical parameters of **4** also agree fairly well with the crystal structure obtained experimentally.[25] The structural change of the PNP ligand from **3** to **4** demonstrates that the cooperation of the PNP ligand and the Ir center promotes the facile cleavage of the H−H bond. The free energy barrier from **3** to $\mathbf{TS_{3/4}}$ is 19.2 kcal/mol. Since **3** is 5.5 kcal/mol above species **2** plus H_2, the transition state $\mathbf{TS_{3/4}}$ is 24.7 kcal/mol with respect to species **2** plus H_2. Experimentally, species **2** reacts with H_2 at low temperature (−78 °C) to generate the product **4**. Thus, the calculated barrier (24.7 kcal/mol calculated at 298.15 K and 1 atm) is somewhat higher than expected. To re-evaluate this barrier, we have optimized the structures of **2** and $\mathbf{TS_{3/4}}$ with several functionals described above (the results are collected in the Supporting Information). The calculated barriers (from **2** to $\mathbf{TS_{3/4}}$) in the solvent (298.15 K and 1 atm) are 15.2 (PBE), 17.0 (TPSS), 19.6 (TPSSh), 20.9 (BMK), and 24.3 kcal/mol (M05), respectively. One can see that M05 functional gives a similar value as B3LYP, but other functionals lead to significantly lower free energy barriers for this step.

From **3**, the transfer of H4 to the amide nitrogen could be another possible route (Scheme 2).[57] Along this route,

(57) Fryzuk, M. D.; Montgomery, C. D.; Rettig, S. J. *Organometallics* **1991**, *10*, 467–473.

Scheme 4. Qualitative Analysis on the Products of the Reaction of D_2 with the Complex (PNP)Ir(C_6H_5)[a]

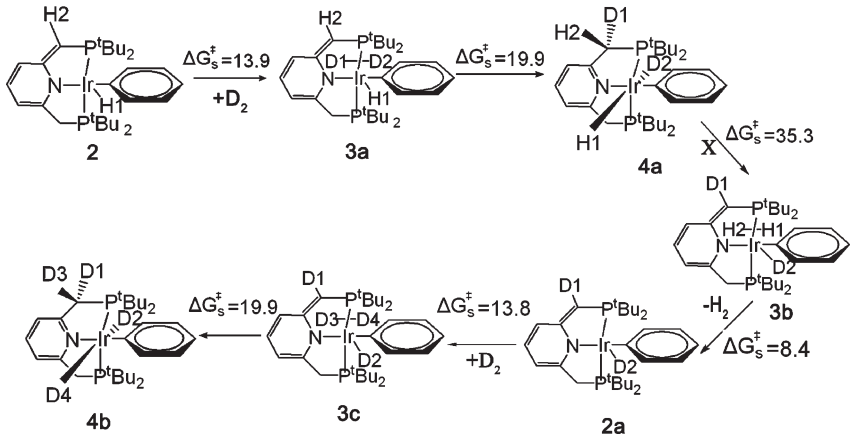

[a] The calculated free energy activation barriers (in kcal/mol) in the solvent for all steps are given for analysis.

the intermediate **5** is produced via the transition state $\mathbf{TS_{3/5}}$, and then this proton (H4) may further migrate through some steps to the benzylic position to yield the final product **4**. Nevertheless, the barrier from **3** to $\mathbf{TS_{3/5}}$ is calculated to be 23.2 kcal/mol, and species **5** is thermodynamically less stable than **3** by 21.2 kcal/mol (Figure 2). Hence, in comparison with the route via $\mathbf{TS_{3/4}}$, the route through the intermediate **5** is energetically disfavored. The H−H bond is most likely to be cleaved with the cooperation of the benzylic carbon of the PNP ligand and the Ir center.

One may wonder whether species **4** could reductively eliminate one of the hydrides and the phenyl ring to form benzene and species **6**. This process is exothermic by 18.9 kcal/mol. In the transition state, $\mathbf{TS_{4/6}}$, the Ir−H3 and C3−H3 distances are 1.655 and 1.405 Å, respectively. Since this reductive elimination step has a free energy barrier of 39.0 kcal/mol, the final product is species **4**, rather than the thermodynamically more stable products **6** and benzene.

3.2. The Potential Energy Surface of the Pathway II. The schematic picture of pathway II is displayed in Scheme 3. This pathway is initiated by the oxidative addition of dihydrogen to the Ir center to form the cis-dihydride intermediate **8**, and then one of the hydrides may migrate to the amide nitrogen atom to form an intermediate **9**. Next, one of the benzylic hydrogens may transfer from the opposite side of the hydride ligand to the metal, resulting in species **5**. Finally, the nitrogen-bound hydrogen will migrate to the benzylic position (possibly via two successive steps) to generate the product **4**.

The optimized structures of some stationary points are presented in Figure 3(a), and the corresponding free energy profile is displayed in Figure 3(b). First, the oxidative addition step of H_2 to produce the cis-dihydride complex **8** via $\mathbf{TS_{1/8}}$ is endothermic by 8.1 kcal/mol, with a barrier of 21.4 kcal/mol. In **8**, two Ir−H bonds are 1.588 and 1.591 Å, respectively. The Ir−N bond is lengthened from 2.130 Å in **1** to 2.160 Å, and the PNP ligand is markedly distorted. Next, the H4 transfer to the amide nitrogen via $\mathbf{TS_{8/9}}$ involves a barrier as high as 54.6 kcal/mol. In **9**, the Ir−N bond (2.248 Å) is quite weak, and the formation of the N−H bond (perpendicular to the pyridine ring) results in the dearomatized structure of the pyridine ring. Due to these structural changes, **9** is a very unstable species, being 43.3 kcal/mol above the reactants (**1**+H_2) and 7.4 kcal/mol higher than $\mathbf{TS_{1/2}}$ (the highest point on the pathway I). Hence, without further exploring the potential energy profile of other subsequent steps along this pathway, one can conclude that this reaction pathway is unlikely to be involved in the H−H activation by the reactant **1**.

3.3. Possible Explanations of Experimental Facts. From the comparison of two potential energy profiles obtained for pathway I and pathway II, it is clear that the reaction is most likely to proceed via pathway I. In the following part, we will show that this mechanism can give reasonable explanations for the experimental facts. First, the reaction of H_2 with **1** at room temperature leads to only the trans-dihydride product **4**. As shown in Figures 2 and 3(b), the formation of the trans-dihydride product **4** is thermodynamically favorable in the solvent, with the free energy change of −8.2 kcal/mol. In contrast, the cis-dihydride complex **8** is 16.3 kcal/mol above the trans-dihydride product **4** in the solvent. By comparing the barriers of several steps along pathway I, one can see that the proton transfer from the benzylic position to the Ir center to form the Ir(III) intermediate **2** is the rate-determining step with a barrier of 35.9 kcal/mol (or 30−35 kcal/mol from calculations with several other functionals). This proton transfer step with a relatively high barrier may occur via a hydrogen tunneling process. The formation of the molecular hydrogen complex **3** and the H_2 activation step from **3** to **4** are relatively facile, with barriers of 13.8 and 19.2 kcal/mol, respectively. Thus, the calculated free energy profile is in reasonable agreement with the experimental conditions, and the experimental fact that only the trans-dihydride product **4** is observed. Furthermore, the calculated free energy profile of pathway I can also account for another experimental fact that the reaction of D_2 with **1** only yields the product, (PNP)Ir(H)(D)(C_6H_5) (**4a**, Scheme 4), with one deuterium being incorporated into the benzylic "arm" (rather than the trans-dideuteride complex, (PNP)Ir(D)(D)-(C_6H_5)). Although the free energy change for the reaction of **4a** with D_2 to form the trans-dideuteride complex (**4b**) and H_2 is −0.6 kcal/mol, the free energy barrier for the formation of the molecular hydrogen intermediate **3b** from **4a** is quite high (35.3 kcal/mol). Thus, species **4b** is difficult to be formed at room temperature. If

the reactant **1** reacts with D_2 at elevated temperatures, it may be possible to observe the trans-dideuteride complex **4b**.

4. Conclusions

We have performed detailed density function theory calculations to investigate the molecular mechanism of the activation of H_2 by the (PNP)Ir(C_6H_5) complex. The potential energy profiles of two possible pathways have been explored. The solvent effect is considered using the PCM model with benzene as the solvent. Our calculations show that the reaction is most likely to go though the following route: first, one of the benzylic hydrogens in the PNP ligand transfers to the Ir center to form an Ir(III) hydride intermediate with the dearomatized PNP ligand; second, H_2 is coordinated to the metal of this Ir(III) intermediate to form an molecular hydrogen complex; finally, with the assistance of the benzylic carbon of the PNP ligand, the activated H−H bond is heterolytically cleaved to produce the final trans-dihydride product, in which the PNP ligand is rearomatized. The first proton transfer step is rate-limiting with a barrier of 35.9 kcal/mol in the solvent (or 30−35 kcal/mol from calculations with several other functionals). This proton transfer step may occur via a hydrogen tunneling process. Thus, the H_2 activation by the Ir(I) reactant is not a typical oxidative addition reaction. In fact, H_2 is activated by a key Ir(III) hydride intermediate. In summary, both the Ir center and the PNP ligand play active roles in the H_2 activation by the (PNP)Ir(C_6H_5) complex. The above molecular mechanism could provide reasonable explanations for available experimental facts. The results from this study may be also useful for understanding the ligand−metal cooperation in other transition-metal complexes with "pincer" ligands.

Acknowledgment. This work was supported by the National Natural Science Foundation of China (Grant Nos. 20625309 and 20833003) and the National Basic Research Program (Grant No. 2004CB719901).

Supporting Information Available: Electronic energies, Gibbs free energies, and Cartesian coordinates of all stationary points and optimized structures of some species with other functionals. This material is available free of charge via the Internet at http://pubs.acs.org.